Very fast charging of low-resistance lead/acid batteries

Eugene M. Valeriote and Daniel M. Jochim
Cominco Ltd., Product Technology Centre, Mississauga, Ont., L5K 1B4 (Canada)

Abstract

Preliminary results are reported which were obtained using a Norvik Minit-Charger™ to rapidly charge low-resistance lead/acid batteries. In initial work, the Minit-Charger was used for ultrafast charging of both flooded and recombination, hybrid and antimony-free designs. Charging was carried out at up to the *C*/5 rate. For the flooded batteries, only modest temperature rises occurred. For a recombination battery, 40% of the previous discharge could be returned at very high efficiency within 6 min and 80% within 16 min with essentially complete recharge in 2 h with an acceptable temperature rise. Temperature rises were, however, greater for the recombination batteries, presumably because of lower heat capacities and poorer heat dissipation characteristics. Work is continuing to optimize the charger parameters, particularly for electric vehicle applications. Preliminary indications are that very fast and efficient recharging of lead/acid batteries is possible but that starved-electrolyte absorbed glass mat batteries need to be designed both for low resistance and to maximize heat dissipation and heat capacity.

Introduction

At the 5th ILZRO International Lead/Acid Battery Seminar in Washington, May 1991, some preliminary results were presented [1] on very fast charging of nickel–cadmium and lead/acid batteries. As was explained, very fast charging meant 5 to 10 min for nickel–cadmium and 10 to 20 min for lead/acid for a substantially complete recharge of a deeply-discharged cell or battery. The results presented then were obtained by Norvik Technologies, the developer of the Minit-Charger™ (Norvik Technologies Inc., Mississauga, Ont.), and by INCO (INCO Ltd., Mississauga, Ont.); they were primarily related to nickel–cadmium cells, in view of INCO's interest in that system, and because very fast charging is well suited to the relatively low resistance of nickel–cadmium cells, and to their endothermal charging characteristic, even at fairly high charging currents.

For a sub-C nickel–cadmium cell (Fig. 1) a continuous cooling process was seen during charging at 6 A, which was the *C*/5 rate, although there was heating during the discharge. During charging, the A h removed in the previous discharge were completely returned and the accompanying cooling maintained the cell within a stable range of temperatures, between 30 and 40 °C, with continuous cycling. The lower curve shows the accumulated charge passed out of and into the cell (multiplied by 10, and plotted against the left-hand *Y*-axis, i.e., a discharge of 1 A h). After removal of about 80% of the nominal capacity, there was complete return of charge removed, with very little overcharge and at a very high efficiency, within 15 min; in fact, well over 90% had been returned within 10 min.

With still smaller cells and a Minit-Charger with a higher current capability, essentially complete charge could be obtained within about 10 min with a peak-charging

0378-7753/92/$5.00

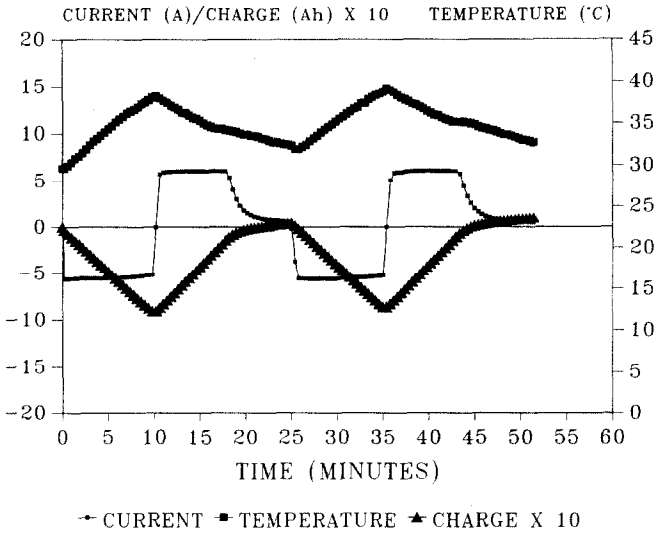

Fig. 1. Cycle data for sub-C (1.2 A h) Ni–Cd cell charging, using a small Norvik Minit-Charger™.

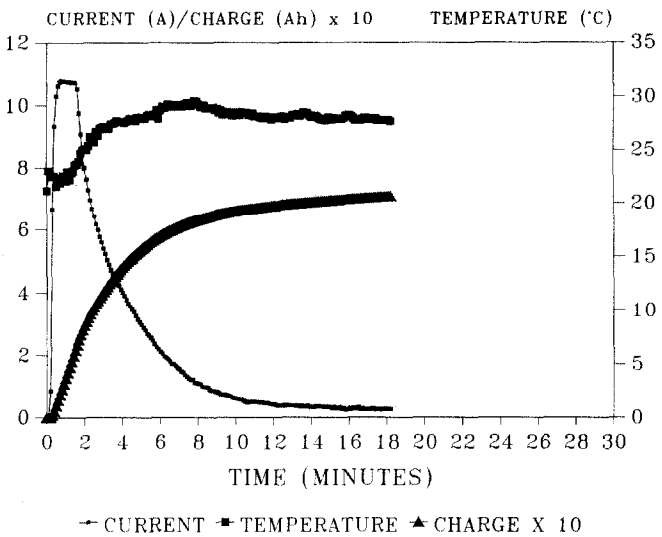

Fig. 2. Charging of a half-sub-C (0.65 A h) Ni–Cd cell with $V_{REF} = 1.50$ V/cell (higher output Minit-Charger™ than for Fig. 1).

current at the *C*/15 or 4 min rate (Fig. 2). Although, in this case, heating occurred during recharge, the temperature increase from initially room temperature to only 30 °C was still quite modest.

Some preliminary results were also presented [1] for lead/acid batteries which, while not quite as outstanding as nickel–cadmium, nevertheless appeared very promising. Only a prototype charger was available at that time and very few runs had been made. In particular, there had been little attempt to determine the efficiency of the recharge

by doing full capacity discharges before and after each charge and we expressed the intention of doing further work at Cominco to evaluate the charger more fully.

In the previous paper the heat-producing mechanisms were also discussed and the reversible thermodynamic heat change was considered, as well as the irreversible charge-transfer overvoltage and resistive heating. It was shown, in a schematic way for a 12 V battery with a 5 mΩ resistance (therefore, five-sixths of a mΩ/cell) and an assumed charge-transfer overvoltage characteristic, that, before gassing begins, by far the largest component of heat production was resistive heating. If the charge were allowed to proceed into gassing at very high currents, the heat produced by the recombination process would become an equally important source of heat. Heat generated by charge-transfer overvoltage or by the reversible heat of reaction was relatively minor. It was concluded that the key components to minimizing temperature increase, therefore, were to minimize battery resistance and gas recombination. Particularly in a valve-regulated lead/acid battery, this means avoiding overcharge since, in a vented battery, some of the heat produced by the recombination reaction can be carried out of the battery by the gas or vapour that escapes.

So far, the main reason for reducing lead/acid battery resistance has been to get high cranking rates. High discharge rates mean high acceleration for an electric vehicle. The low resistance can mean an extension of the vehicle's range, if it facilitates a very fast recharge, even if only up to 80 or 90% of full charge. This could open up substantial new markets for lead/acid batteries in electric vehicle propulsion and for that reason Cominco became involved with Norvik to extend the work that they had already started, because of the growing interest in these batteries, particularly for electric vehicle applications. We wanted first to determine the limits on charging rates of batteries of various low-resistance designs and especially for recombination batteries, which Norvik had not investigated.

Experimental

A computer monitoring and control system was set up based on Viewdac™ software (Asyst Software Technologies, Inc., Rochester, NY) on a 386 SX PC. Initially, the application programmes were written to control a programmable power supply and an electronic load, and a series of charges and discharges was carried out with conventional charging to establish the Peukert characteristics (Fig. 3) for the batteries that would later be evaluated using the Minit-Charger. The batteries selected had capacities in the range of 50 to 60 A h at the 2 to 3 h rate. The first four represented in Fig. 3 were of four different types. One was a Group 24 absorbed glass mat (AGM) recombination battery which had antimonial positive plates and was a commercial RV-Marine deep-cycling battery. The second was a nonantimonial Group 24 recombination battery, again with absorbed glass mat design. Both of these batteries had low internal resistance, of the order of 3 to 4 mΩ when fully charged, as measured by a 1000 Hz a.c. milliohmmeter. The third battery type was a Group 27 recombination gelled battery with a somewhat higher internal resistance and the fourth and fifth were two flooded starting-lightning-and-ignition (SLI) batteries, one with low resistance and the other with a higher resistance. The capacity of the gelled battery, which has not yet been evaluated for fast charging, is somewhat higher than those reported here. The other four capacities were tightly grouped around 50 A h at the 3 h rate. Two other battery types have been ordered but have not yet been put into the test programme. One is a flooded low-resistance pseudo-bipolar design, and the other is a nonantimonial,

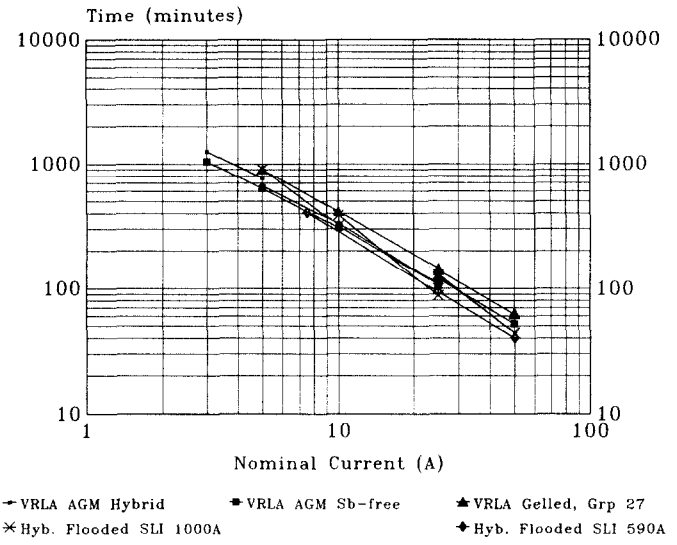

Fig. 3. Peukert plot for five test batteries prior to fast-charge cycling.

TABLE 1

Battery resistances at various depths-of-discharge, after cycling

Battery type	R–Fully charged (mΩ)	R–80% DOD (mΩ)	R–100% DOD (mΩ)
Hybrid flooded SLI 1000 CCA[a]	3.45	3.65	5.02 (6.9)[b]
VRLA[c] AGM hybrid	3.15 (3.45)	6.4	9.15
VRLA AGM antimony-free	3.20	4.02	9.40
Hybrid flooded SLI 590 CCA	4.7		8.25
VRLA gelled	5.15		

[a]CCA: cold cracking rating in A (30 s, 7.2 V, −18 °C) defined by the Battery Council International.
[b]Values in brackets were obtained after substantial cycling; values not in brackets were obtained during the first ten cycles.
[c]VRLA: Valve-regulated lead/acid.

absorbed glass mat, low-resistance recombination battery, but this time with prismatic construction, rather than cylindrical cells as in the antimony-free battery examined for this paper.

The measured battery resistances at various depths-of-discharge (DOD) are shown in Table 1. The high-CCA flooded battery and the two recombination batteries both had relatively low resistances when fully charged, which increased only modestly until approaching full discharge and then increased more abruptly. Values in brackets were measured after a substantial amount of cycling. The values not in brackets were taken after the Peukert characterization and, sometimes, a few fast charge cycles. The software and experimental system began operating smoothly only about six weeks prior to writing this paper and so, substantial data are reported here only on the first four batteries in this Table.

The experimental parameters that we have varied so far are shown in Table 2. The only control over the internal resistance is in the choice of battery. The I^2R

TABLE 2

Parameters investigated

Battery resistance/design
Charging current limit
Charging reference voltage (V_{REF}) limit
Charging voltage temperature compensation
Depth of previous discharge
Location of temperature sensors

heating, however, will also be strongly affected by the charging current and so a number of charging currents from 100 up to the 300 A maximum output of the charger are being investigated. The principle of operation of the charger is to maintain a constant current until the resistance-free voltage (V_{REF}) applied to the battery increases to the selected set point. The resistance-free voltage is maintained by periodically interrupting the charging current to measure the battery voltage after a few milliseconds of voltage decay and maintaining this resistance-free voltage value constant by means of electronic feedback circuits. Once the selected reference voltage is reached, the current is then decreased in steps, and the voltage is allowed to rise at the new constant current until the reference voltage is reached again. The choice of reference voltage is the second, and perhaps the most important, parameter being studied. If too low a reference voltage is selected, the battery will not be fully charged within a reasonable period of time, if at all. If too high a value is selected, there will be excessive gassing or, in a recombination battery, excessive heat generation due to the recombination reaction. The reference voltage selected should normally be close to the constant float or charging voltage recommended by the manufacturer. Since the temperature may increase during the charging process, a temperature-compensation coefficient, to reduce V_{REF} with increasing temperature, can be selected by varying a potentiometer. Another factor, which will effect temperature rise, is the depth of the preceding discharge. This, in turn, determines, not only initial ohmic heating, but also the amount of charge to be returned and, therefore, the duration of the high-current ohmic heat production period. Once the optimum charging parameters have been established, life-cycling endurance testing will be the next phase. Some indication of the effects of the charging parameters on cycle life, however, can be obtained from the temperature increases that occur for various charging conditions. The general approach followed up to now is to determine what conditions cause the temperature to increase to 50 to 60 °C both internally and on the insulated surface of a battery sidewall. The temperature rise is determined not only by the amount of heat produced by the charging process but also by the rate of heat dissipation and the heat capacity of the battery.

An instrumented battery contained two temperature probes, one a thermocouple inserted to the bottom of a capillary and sealed inside the battery, with the capillary inserted into the electrolyte or separator. A thermocouple was also placed underneath insulation on the sidewall of the case, and a hole was drilled into the bottom of the negative post into which another thermocouple could be inserted. A pressure transducer was used, also sealed into the cover, to measure the internal pressure of the battery. No pressure results are reported here because of the difficulties in getting good pressure data during the charge portion of the cycle. This was a result of interference from the switching power supply used in the charger. A current-loop pressure transducer has been just obtained and the switching noise has been reduced for future work.

The voltage applied to the battery terminals and other variables could also be recorded, those such as plate potentials relative to a reference electrode and V_{REF} (controlled by the charger). The computer was used to control the electronic load by sending an analog signal during the discharge and to monitor the analog signals from the sensors but it does not control the Minit-Charger, except to turn it on and turn it off. Once the charger had been turned on, the charge was terminated either by the computer-programmed (or Minit-Charger hardware set) time period selected or if the charging current decreased and remained at a very low programmed value. Although the Norvik charger has provisions for inclusion of equalization charging periods and float charging, which could be selected by potentiometer settings inside the charger and by pushbuttons on the panel, these were not used for the purposes of the work reported here.

Results

For the first battery studied, temperature rises inside this hybrid absorbed glass mat recombination battery initially exceeded expectations (Fig. 4). Those expectations were based on the work reported last year showing only 10 to 15 °C temperature rises. Those results, however, were obtained with flooded batteries and following lesser amounts of discharge than for the work reported here. After a 100% DOD at the 3 h rate, an internal battery temperature (Temp int) was observed which exceeded 70 °C, when the charge current was limited to 200 A at a V_{REF} of 2.45 V with no temperature compensation. Also shown in Fig. 4 are the integrated charging current, rising to about 60 A h, the case temperature (Temp ext), and ten times the battery voltage, plotted on the left-hand scale. The temperature was also monitored using a thermocouple placed in a hole drilled in the battery post. The post temperatures are not shown here because, for a recombination battery with a thermally noninsulated post, the post was much cooler than either the inside of the battery or the insulated

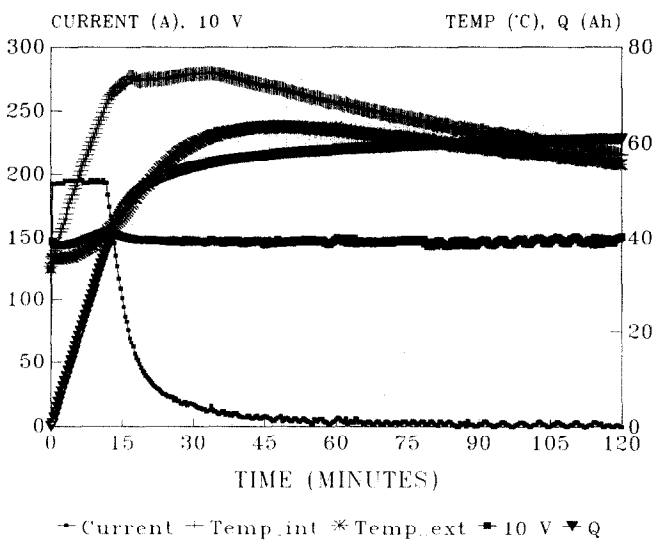

Fig. 4. Charging of VRLA hybrid AGM battery with $V_{REF} = 2.45$ V, no temperature compensation and 200 A limit following a 100% DOD.

outside of the case. It can be seen that the case temperature variation lagged substantially behind the internal temperature with the two converging after 1 h or so of charging. It was apparent that the temperature of the post was being controlled primarily by the ambient temperature. In order to get post temperatures similar to the internal temperatures, the post itself had to be insulated from the environment.

For the second battery examined, the nonantimonial cylindrical-cell configuration, very large temperature increases were again observed (Fig. 5) under the experimental conditions originally chosen (for cycle 38),but in this case the high temperature may have been a spurious effect, as will be explained. For these runs the temperature compensation was set at 3 mV/°C. Later, this was altered to 4 mV/°C, a value for VRLA batteries taken from a recent paper by Berndt [2]. A higher reference voltage was used for cycle 38 than for cycle 41. For this battery, the insulated post was used to indicate the internal temperature, because of difficulties in placing a thermocouple inside the battery itself. Initially, when the charging current was turned on, there was a high-temperature transient which was probably not indicative of interior battery temperatures. Only by reducing the limiting charging current to about the *C*/2 rate was it first possible to keep the temperature of these two batteries within an acceptable range. What is odd about Fig. 5, where results are shown for both cycle 38 and cycle 41, is that the post temperature rise at the lower current limit (150 A, which is about the *C*/3 rate) was more than at the 200 A (*C*/4) rate. The charge in cycle 38 terminated itself at 34 min, since it was programmed to stop when the case temperature rose to 60 °C. The higher reference voltage, promoting more recombination, was probably the reason for the case temperature getting so high. Another probable factor was that, between these two runs, the posts and clamps were abrasively cleaned reducing the connector contact resistance by a factor of about 10 from 0.2 to about 0.02 mΩ. At 200 to 250 A, the resistive heating for a 0.2 mΩ contact resistance is about 10 W.

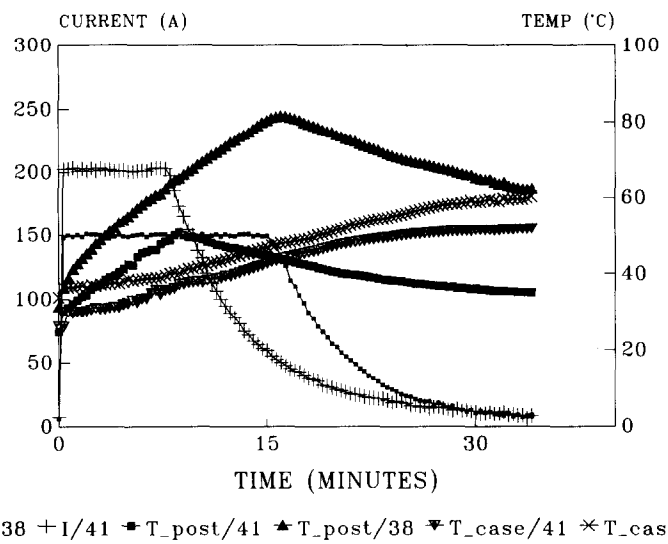

Fig. 5. Charging of VRLA antimony-free AGM battery with cylindrical cells following a 100% DOD; cycle 38: 150 A limit, V_{REF} = 2.45 V; cycle 41: 200 A limit, V_{REF} = 2.45 V; 3 mV/°C temperature compensation. Temperatures have been measured in negative post and on case wall.

This could cause a substantial increase of temperature for the low-heat-capacity metal of the post and, indeed, the posts felt very warm to the touch during the high current period of cycle 38. Cycle 41 is discussed further below.

Between cycles 38 and 41, in order to determine the reasons for unexpectedly-high temperature increases, a third battery with a flooded design was studied. The temperature rises for this battery under similar, or even more aggressive, charging conditions were much smaller. In Fig. 6 are shown charges at 255 and 150 A limits. In the 255 A (*C*/5) case, the electrolyte temperature rose to a maximum only about 10 °C above the starting temperature. The post temperature got slightly warmer initially but cooled faster because of the thermal path from the post to the copper bus bars. Although the post was insulated, the copper and shunt connected to it were not at that stage. The 80% DOD was 80% of nominal but 100% of actual. This particular battery was a 23-plate-per-cell high CCA battery not designed for deep cycling and it had lost substantial capacity during the Peukert characterization even before it had experienced any fast charging. The internal temperature measured in the electrolyte above the plates was not substantially different from the temperature monitored on the outside of the battery case and so the curve showing internal temperature also fairly represents the case temperature. Eleven cycles have since been done on a 13-plate-per-cell Group 34 hybrid SLI battery with better capacity retention and similarly modest temperature increases (Fig. 7).

The observations suggest that the thermal contact between the electrolyte and the battery case is much better in a flooded battery than in a starved electrolyte battery, as one might expect. With the data obtained so far, it is not clear how important differences in heat capacities between the flooded and the AGM batteries are. If these are substantially different, then the same amount of heat would produce a much smaller temperature rise for the battery with higher heat capacity.

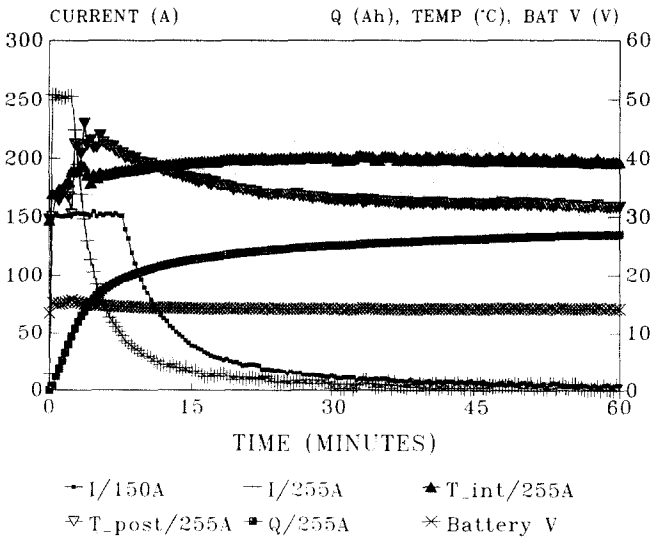

Fig. 6. Charging of SLI hybrid flooded 1000 CCA battery after an 80% DOD; V_{REF} = 2.45 V, 6 mV/°C temperature compensation; internal and post temperatures, charge input and battery voltage with 255 A charging limit; currents with 150 and 255 A limits.

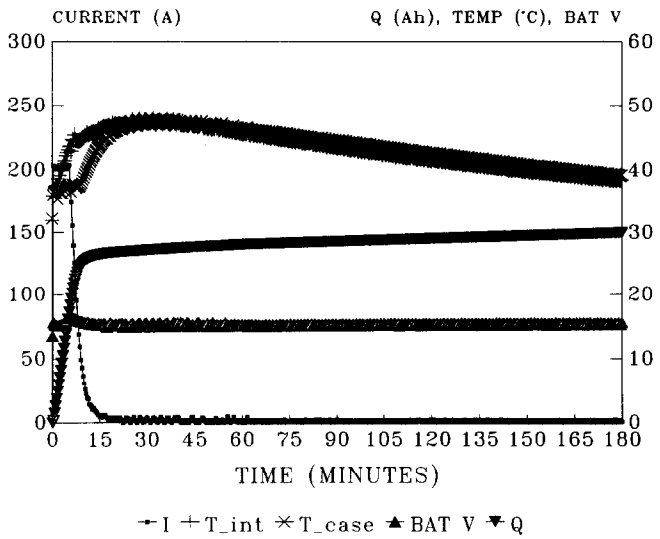

Fig. 7. Charging of SLI hybrid flooded 590 CCA battery after 80% DOD; V_{REF} = 2.67 V, 6 mV/°C temperature compensation; current, internal and case temperatures, charge input and battery voltage for 3 h charge.

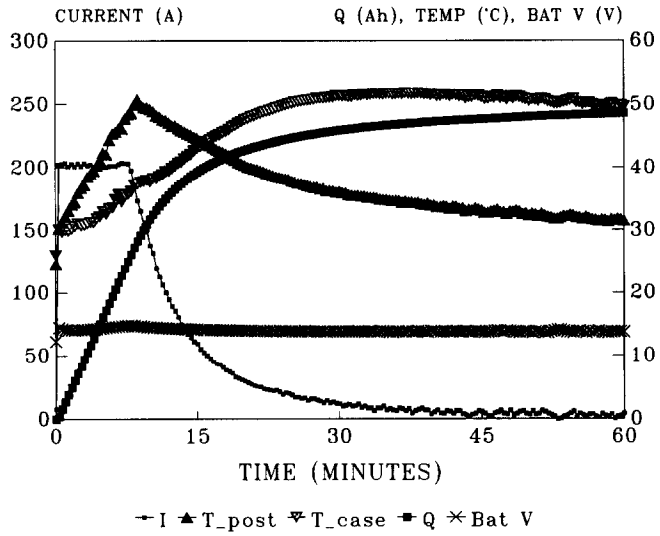

Fig. 8. Charging of VRLA antimony-free AGM battery after 100% DOD; cycle 41: V_{REF} = 2.35 V, 3 mV/°C temperature compensation; current, post and case temperatures, charge and battery voltage for first hour of charge.

Results for cycle 41, for the antimony-free recombination battery, with the terminals cleaned to reduce the connector resistance, are shown in Fig. 8. The current was limited to 200 A, with the lowest V_{REF} investigated to date (2.35 V). The temperature in the insulated post peaked near 50 °C, just after the current started to drop, but then cooled to less than that of the case after about 15 min, while the case peaked

at about the same temperature but about a half-hour after the peak post temperature. The battery voltage will also peak, as shown, just as the current starts to drop, since the voltage applied to the battery is $V_{REF}+IR$ and from this point on the IR component decreases.

The preceding 100% discharge was 50.65 A h and it is apparent that almost all was returned within 1 h. As an indication of how efficient the recharge was for the same cycle, Table 3 shows that the following 100% discharge was 51.4 A h. The charge terminated after 78.4 min, when 50.1 A h had been returned, because of the low charging-current cutoff programmed. In the last 15 min, only 0.5 A h (1% of capacity) was returned and, in the last 5 min, only 0.1 A h, so very little more would have been returned had the charge been extended. Thus, the recharge was very efficient approximately 100% within the 1 to 2% error in measuring and integrating the charging current. Here we see that 40% was returned in the first 6 min, 50% by 7.7 min and 80% by 16 min, while the remaining 20% took another hour.

After cycle 41, the charging parameters were varied further and methods were improved. At over 50 cycles there was no indication of capacity degradation. In

TABLE 3

Charge returned and efficiencies

Previous discharge				50.65 A h	at 25 °C
Partial charge (% of 50.1 A h)	40	50	80	90	100
Time (min)	6.0	7.7	16.0	26.0	78.4
Last 5 min	0.1 A h		Last 15 min	0.5 A h	
Following discharge				51.38 A h	at 24 °C

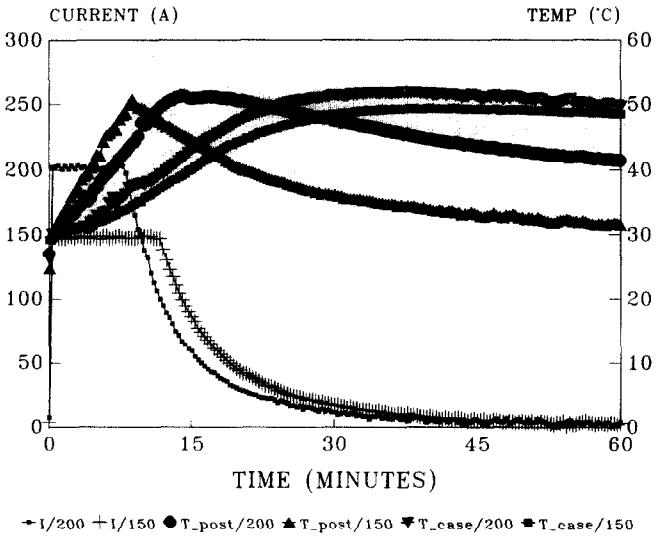

Fig. 9. Charging of VRLA antimony-free AGM battery after 100% DOD; cycle 41: V_{REF}= 2.35 V, 3 mV/°C temperature compensation; current and post and case temperatures.

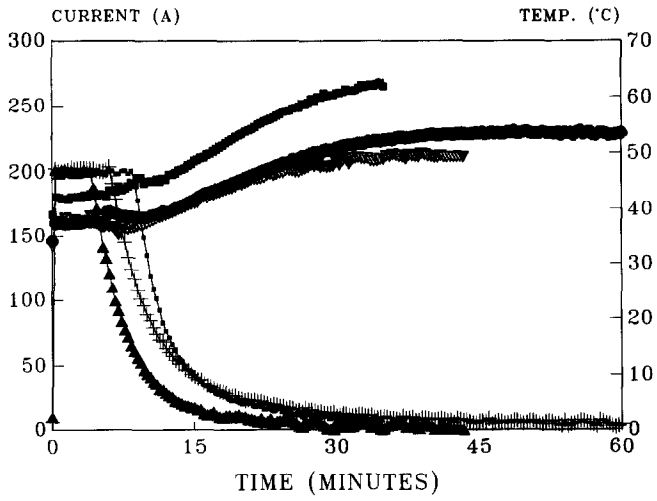

Fig. 10. Charging of VRLA hybrid AGM battery: cycle 16: $V_{REF}=2.40$ V, no temperature compensation; cycle 25: $V_{REF}=2.50$ V, no temperature compensation, after 80% DOD; cycle 42: $V_{REF}=2.50$ V, 3 mV/°C temperature compensation after 50% DOD.

Fig. 9, we compare charges at 200 A and 150 A limits but with the insulation of the post improved so that about the same peak post temperature was reached at the lower current as had been the case at the higher current with less post insulation. The post cooling has obviously been retarded by the better insulation. The case temperatures showed the expected lesser temperature rise at the lower current, although the difference is not great.

The effects of other parameters affecting heating are shown in Fig. 10 for the other recombination battery. As the reference voltage was decreased from 2.50 to 2.40 V, (in both cases with a 200 A limit) the maximum current was delivered for a shorter period of time following a prior 80% DOD, and even shorter after a 50% DOD, and temperature rises were in the order of the high-current charging durations. Note that the starting temperatures were high for these runs and the temperature rises were only 15 to 30 °C. Although the temperature at $V_{REF}=2.40$ V, for example, rose to 54 °C after the 80% DOD, it began at 35 °C, so the temperature change was just under 20 °C. An 80% DOD is probably a more realistic real-life condition for fast charging of electric vehicles than 100% since few people will want to risk a 100% discharge unless they are very close to a charging station. By following the end-of-discharge voltage for 80% discharges, it was also possible to infer high recharge efficiencies.

Conclusions

This work has just begun and it is too early to be able to give definitive answers to all the questions that remain about the capabilities and effects of very fast charging. There are some preliminary conclusions that can be drawn, however:

(i) Very fast and efficient recharging of lead/acid batteries is possible.
(ii) Connector contact resistances must be minimized.
(iii) Temperature increases appear acceptable for flooded battery designs.

(iv) Starved-electrolyte batteries will need to be designed, not only for low resistance, but also for maximum heat dissipation. As well, heat capacities may need improvement if such starved-electrolyte designs are to achieve as wide a range of applications as appear likely for flooded batteries. This will be particularly important for applications where valve-regulated batteries are preferred, as is the case for vehicle propulsion. That part is a challenge for the battery manufacturers and will probably require the use of both different battery geometries and also of more heat-conductive battery materials and innovative ways to extract heat.
(v) Further optimization of charging parameters and battery design are needed and appear worthwhile.

Future work

We are hoping to establish the optimum parameters for fast recharge of individual laboratory batteries in order to apply the principle to the much larger battery required for electric vehicles. At the same time as we carry out the laboratory testing, we will be instrumenting the modules within the battery pack on our electric van in order to determine the nonuniformity of the modules, voltages and temperatures, so that we will know which modules, or which combinations of modules, to use as pilot cells to permit very rapid recharging and, therefore, vehicle range extension in a real vehicle application. We also plan to do more cycle-life testing once the optimum parameters are determined.

References

1 E. M. Valeriote, J. K. Nor and V. A. Ettel, *Proc. 5th Int. Lead/Acid Battery Seminar,* International Lead Zinc Research Organization (ILZRO), Inc., Research Triangle Park, NC, 1991, pp. 93–122.
2 D. Berndt, *Proc. 10th Int. Telecommunication Energy Conf., San Diego, CA, Oct. 30–Nov. 2, 1988,* Institute of Electric and Electronic Engineers, Piscataway, NY, 1988, pp. 89–96.